ISSN 1547-4771, Physics of Particles and Nuclei Letters, 2013, Vol. 10, No. 5, pp. 415–421. © Pleiades Publishing, Ltd., 2013.
Original Russian Text © D.A. Artemenkov, A.A. Bezbakh, V. Bradnova, M.S. Golovkov, A.V. Gorshkov, P.I. Zarubin, I.G. Zarubina, G. Kaminski, N.K. Kornegrutsa, S.A. Krupko, K.Z. Mamatkulov, R.R. Kattabekov, V.V. Rusakova, R.S. Slepnev, R. Stanoeva, S.V. Stepantsov, A.S. Fomichev, V. Chudoba, 2013, published in Pis'ma v Zhurnal Fizika Elementarnykh Chastits i Atomnogo Yadra, 2013, No. 5(182), pp. 679–690.

PHYSICS OF ELEMENTARY PARTICLES AND ATOMIC NUCLEI. EXPERIMENT

Exposure of Nuclear Track Emulsion to ^{8}He Nuclei at the ACCULINNA Separator

D. A. Artemenkov[a], A. A. Bezbakh[a], V. Bradnova[a], M. S. Golovkov[a], A. V. Gorshkov[a], P. I. Zarubin[a], I. G. Zarubina[a], G. Kaminski[a, b], N. K. Kornegrutsa[a], S. A. Krupko[a], K. Z. Mamatkulov[a], R. R. Kattabekov[a], V. V. Rusakova[a], R. S. Slepnev[a], R. Stanoeva[c], S. V. Stepantsov[a], A. S. Fomichev[a], and V. Chudoba[a, d]

[a] *Joint Institute for Nuclear Research, Dubna, Russia*
[b] *Institute of Nuclear Physics, Polish Academy of Sciences, Krakow, Poland*
[c] *South-West University, Blagoevgrad, Bulgaria*
[d] *Institute of Physics, Silesian University in Opava, Czech Republic*

Abstract—Nuclear track emulsion is exposed to a beam of radioactive ^{8}He nuclei with an energy of 60 MeV and enrichment of about 80% at the ACCULINNA separator. Measurements of 278 decays of the ^{8}He nuclei stopped in the emulsion allow the potential of the α spectrometry to be estimated and the thermal drift of ^{8}He atoms in matter to be observed for the first time.

DOI: 10.1134/S1547477113050026

INTRODUCTION

At nuclear energies of a few MeV, it becomes possible to implant radioactive nuclei into the detector material and thus investigate daughter states resulting from their decays rather than the implanted nuclei themselves. For example, decays of light radioactive nuclei can populate 2α and 3α-particle states. The known, though slightly forgotten, possibilities of detecting slow nuclei in nuclear track emulsion are worth considering in this connection. The advantages of this method are the best spatial resolution (about 0.5 μm), the possibility of observing tracks in the complete solid angle, and a record sensitivity range beginning with relativistic singly charged minimum ionizing particles. Nuclear track emulsion allows directions and ranges of beam nuclei and their decay products to be measured, which provides the basis for α spectrometry.

More than 50 years ago, hammerlike tracks of ^{8}Be → 2α were observed in nuclear track emulsion. They resulted from β decays of stopped ^{8}Li and ^{8}B fragments produced in turn by high-energy particles as emulsion nuclei underwent splitting [1]. Another example is the first observation of the 2α + *p* decay of the ^{9}C nucleus via the 2^+ state of the ^{8}Be nucleus [2]. Due to the development of facilities for producing beams of radioactive nuclei, nuclear track emulsion turned out to be an effective tool for studying decays of light exotic nuclei with both neutron and proton excess.

As a first step within this approach, the nuclear track emulsion was exposed to ^{8}He nuclei with an energy of ~60 MeV at the Flerov Laboratory of Nuclear Reactions (FLNR JINR) in March 2012. The features of ^{8}He decays are depicted in Fig. 1 in accor-

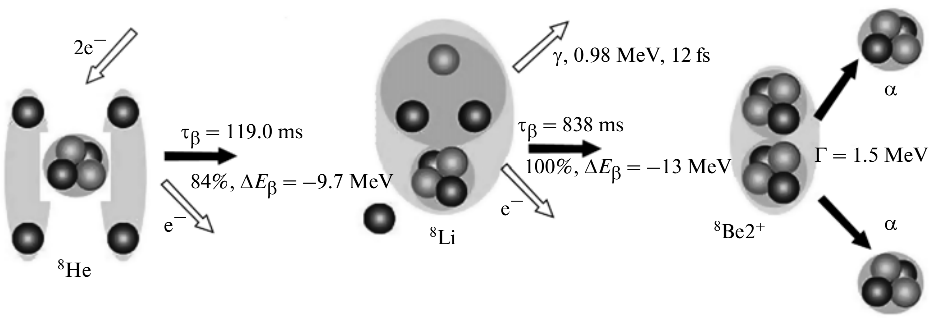

Fig. 1. Scheme of the main cascade decay channel for the ^{8}He isotope. Circles are protons (light) and neutrons (dark). Darker background indicates clusters.

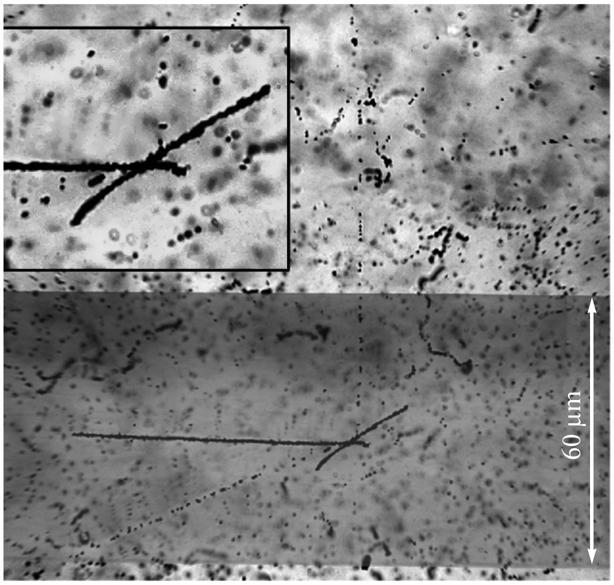

Fig. 2. Mosaic macrophotograph of the hammerlike decay of the ^{8}He nucleus stopped in the nuclear track emulsion (horizontal track). The decay results in a pair of relativistic electrons (dotted tracks) and a pair of α particles (oppositely directed short tracks). The inset shows the enlarged decay vertex. The decay image is superposed on the macrophotogtraph of a human hair 60 μm thick to illustrate the spatial resolution.

dance with [3]. After the ^{8}He nucleus is stopped and neutralized in the substance, the formed ^{8}He atom remains unbound (noble gas) and, as a result of thermalization, can drift in the substance until it undergoes β decay. The half-life of the ^{8}He nucleus is $\tau_\beta = (119.0 \pm 1.5) \times 10^{-3}$ s. This nucleus undergoes β decay to the 0.98-MeV bound level of the ^{8}Li nucleus with a probability of 84% and energy $\Delta E = 9.7$ MeV. Then the ^{8}Li nucleus with its half-life $\tau_\beta = (838 \pm 6) \times 10^{-3}$ s undergoes β decay to the 2^+ level of the ^{8}Be nucleus (3.03 MeV) with 100% probability and energy $\Delta E =$ 13 MeV. Finally, the ^{8}Be nucleus decays from its 2^+ state with the width of 1.5 MeV to a pair of α particles.

Figure 2 shows a mosaic macrophotograph of the decay of the ^{8}He nucleus stopped in nuclear track emulsion (one of several thousand events observed in this investigation). Video records of these decays made with a microscope and a camera are collected on the BECQUEREL site [4]. This work deals with an analysis of the irradiation in question based on the measurements of 278 decays of this type.

EXPERIMENTAL

Nuclear track emulsion was exposed to ^{8}He nuclei with an energy of 60 MeV at the ACCULINNA fragment separator of FLNR JINR [5, 6] (Fig. 3). A beam of heavy ^{18}O ions with an energy of 35 MeV/nucleon and intensity of ~0.3pμA extracted from the U400M cyclotron [7] was used to produce ^{8}He nuclei. The ^{18}O ions bombarded a target of pyrolytic graphite 175 mg/cm^2 thick located in the plane F_1. The target was a disc 20 mm in diameter and 1 mm thick sandwiched between two water-cooled copper plates. The beam spot on the target was shaped with one of the plates used as a collimator 8 mm in diameter. This collimator was also used to tune the primary beam channel to the maximum ^{18}O beam transmission, usually as high as 90%.

The primary beam intensity was measured by two Faraday cups placed in the plane F_1 in front of and behind the collimator. The beam intensity was monitored during exposure by measuring the current on the tantalum foil (4 μm thick) fixed in place in front of the second Faraday cup.

The parameters of the separator tuning for the production and shaping of the secondary ^{8}He beam in the

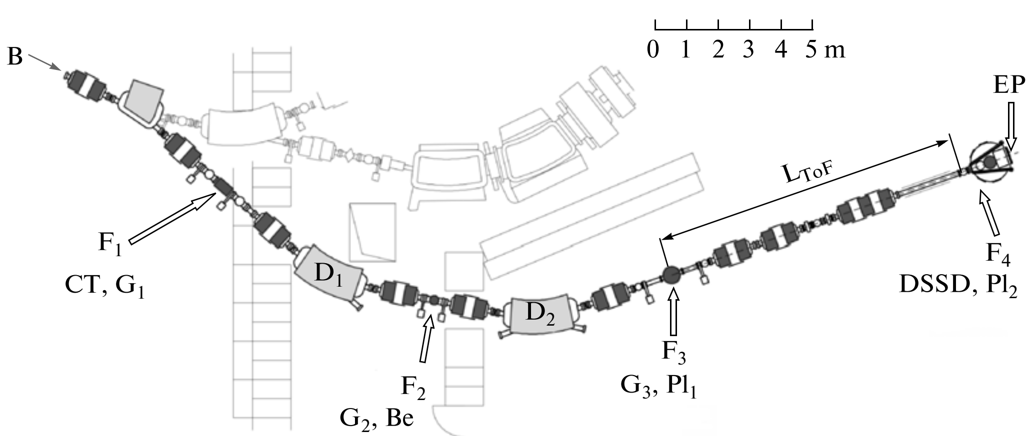

Fig. 3. Scheme showing the production of the 60-MeV ^{8}He beam at the ACCULINNA separator and the location of the nuclear track emulsion pellicles in the focus F_4 during their exposure to ^{8}He nuclei. B is the direction of the primary beam extracted from the U400M accelerator; CT is the carbon target; $F_{1,2,3,4}$ are the focal planes; $G_{1,2,3}$ collimator gaps; Be is the beryllium wedge; $Pl_{1,2}$ are the plastic scintillator detectors; DSSD is the strip silicon detector; L_{ToF} is the time-of-flight measurement path; and EP is the emulsion pellicle exposure place.

achromatic focus F_3 and final focus F_4 were determined from the field calculations for the dipole and quadrupole elements using the TRANSPORT code [8, 9]. The beam composition in the final focal plane F_4 was set and monitored by (i) a gap with the dimensions $X = \pm 5$ mm and $Y = \pm 10$ mm and a beryllium wedge 1000 μm thick in the intermediate plane F_3, (ii) a gap with the dimensions $X = \pm 5$ mm and $Y = \pm 10$ mm in the achromatic focus F_3, and (iii) two identical thin BC418 plastic scintillator detectors 60 × 40 mm in size and 127 μm thick viewed by two photomultiplier tubes on the left and on the right in F_3 and F_4 for the time-of-flight identification of particles and measurement of their energies. These detectors with a temporal resolution of about 0.5 ns (half-width at half-maximum) installed in the straight section 8.5 m long ensured particle energy determination with an accuracy no worse than 1%.

The design of the time-of-flight detector is shown in Fig. 4. A 2-μm-thick foil of aluminized Mylar served as a reflector. Diffuse reflection is provided by the Tyvec light guide. The scintillators were viewed on the left and on the right downstream of the beam by two fast XP2020 photomultiplier tubes, which allowed correcting the signal amplitude and time dependences on the particle entrance point in the detector. The positional resolution of the detector in the horizontal coordinate determined from the relative left-to-right signal amplitude ratio was about 10 mm. The above dependences were especially noticeable and important for the detector in the focus F_4, where the converging secondary beam spot was an ellipse 40 × 30 mm in size.

A position-sensitive silicon detector 1 mm thick with an active area 50 × 58 mm in size and 1.8-mm-wide sensitive strips was installed at a distance of 130 cm from the scintillation detector in F_4 downstream of the beam immediately in front of the vacuum chamber exit window. The silicon detector allowed the beam profile to be determined in two coordinates with an accuracy of 1.8 mm and particles to be uniquely identified by measuring the particle energy loss more accurately than with the plastic scintillator detector. Measured by this detector, the ^{8}He beam profile in the X and Y planes was about 26 mm (half-width at half-maximum). Figure 5a presents an identification picture of the beam of radioactive nuclei obtained by measuring the energy loss of particles in the silicon detector as a function of their time of flight over the path of 8.5 m when the separator was tuned to the maximum ^{8}He beam transmission.

The magnetic rigidity of the dipole magnets D_1 and D_2 $B\rho_1/B\rho_2 = 2.8903/2.829$ T m and the wedge-shaped beryllium absorber (1 mm) with gaps of ±5 mm in maximum dispersion plane F_2 set the following characteristics of the secondary ^{8}He beam in plane F_4: energy 23.8 ± 0.9 MeV/nucleon, intensity ~50 particles/s at a primary beam intensity of ~0.3 $p\mu$A, and ^{8}He enrichment ~80% (Figs. 5b, 5c).

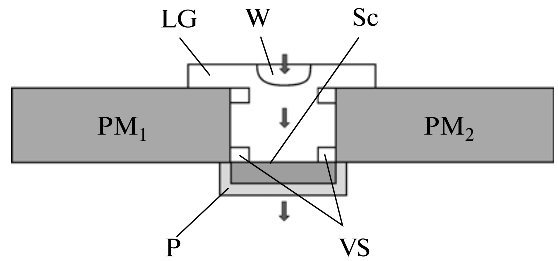

Fig. 4. Schematic view of the scintillation detector for measuring the time of flight of the fragments along the straight section F_3–F_4 of ACCULINNA: W is the beam entrance window covered with a reflector; LG is the total diffuse light guide; SC is the scintillator; $PM_{1,2}$ are the photomultipliers; R is the reflector; VS are vacuum seals.

Considering the detector material inside the vacuum chamber, the Kapton exit window (125 μm thick), and the aluminum plate (3900 μm thick) installed in the air behind the window at a distance of ~2 cm, the calculated energy of the ^{8}He nuclei before their hitting the emulsion assembly was about 59.2 ± 4.5 MeV. Several emulsion pellicles were exposed to the beam with these characteristics. The exposure of each pellicle was about 10 min long, which corresponded to the integral flux of about 4 × 10^4 ^{8}He nuclei.

The emulsion used for exposure (conventionally referred to as series 21) is an analogue of the known BR–2 emulsion recently reproduced at the Mikron factory of the Slavich Company [10], which is sensitive to minimum ionizing relativistic particles. This investigation can be regarded as a calibration of the nuclear track emulsion in a physical experiment.

To choose the optimum observation of ^{8}He stops, emulsion pellicles 9 × 12 cm in size and 107 μm thick produced by splashing onto the glass substrate 2 mm thick were placed in the beam both across it and at an angle to its axis (10 to 20°). The subsequent scanning revealed that the best pellicle for analysis was the one inclined at an angle of 10°. An inclination of the plate resulted in a larger deceleration layer in the emulsion pellicle. It is this pellicle that was used for analysis in this work. Before exposure, the pellicles were wrapped in two layers of black paper 100 μm thick each. The beam nuclei were thus given additional deceleration, especially sensitive at the angle of 10°.

ANALYSIS OF HAMMERLIKE DECAYS

As the pellicle was scanned using an MBI-9 microscope with a 20× lens, the primary search for β decays of ^{8}He nuclei was focused on hammerlike events (Fig. 2). The absence of tracks of a decay electron in the observed event was interpreted as a consequence of the inadequately effective observation of all decay tracks in the emulsion pellicle. The most problematic background for selection by this criterion could arise

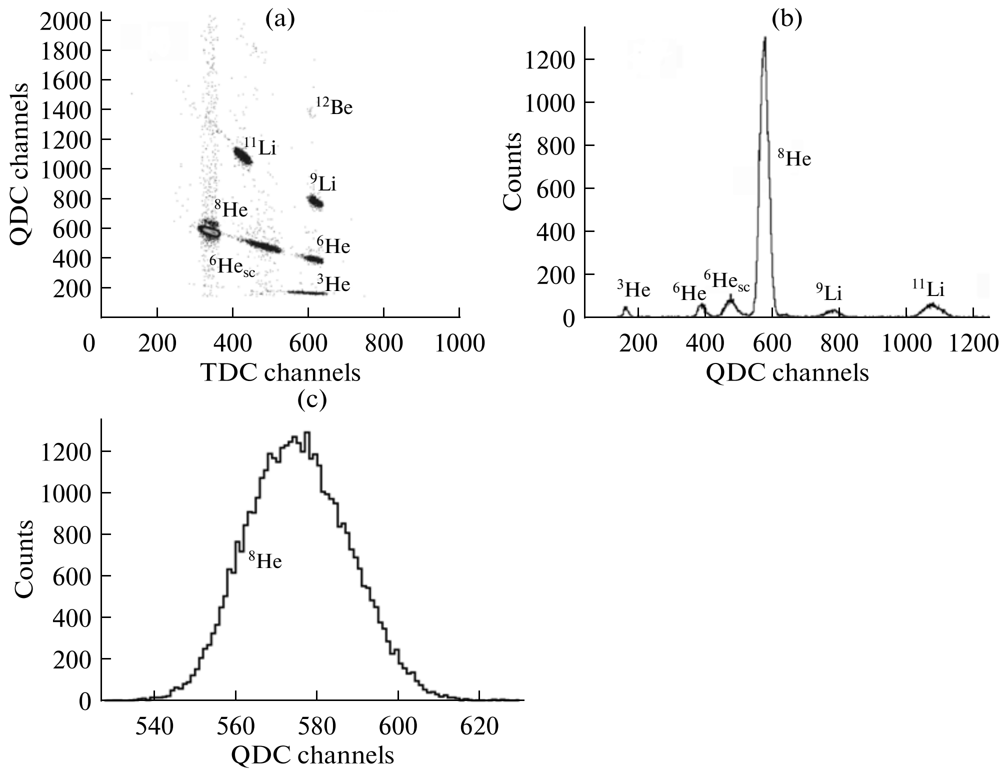

Fig. 5. Composition of the beam produced at the ACCULINNA separator tuned to the ^{8}He isotope from the fragmentation of the ^{18}O nuclei with an energy of 35 MeV/nucleon on the ^{12}C target. (a) Identification of particles by the silicon detector and from the time of flight; (b) spectra of energy lost by all beam particles in the silicon detector 1 mm thick; and (c) energy loss of ^{8}He nuclei alone. The sum of counts in (b) and (c) was used to find the beam enrichment in ^{8}He nuclei.

from decays of ^{8}Li nuclei. However, as follows from Fig. 5a, this isotope is not observed. Beta decay of stopped ^{9}Li nuclei with the formation of ^{8}Be and the emission of a delayed neutron (probability ~50%) could also meet the above criterion, but the admixture of these nuclei is small (Fig. 5a). In addition, for the decay of the ^{8}Be 2^{+} state to be hammerlike, it must populate the ^{9}Be level at an energy no lower than 4.7 MeV. Otherwise, the decay proceeds via the 0^{+} ground state of the ^{8}Be nucleus and is therefore hardly observable even in emulsion. Thus, the background from decays of ^{8}Li and ^{9}Li nuclei could be ignored.

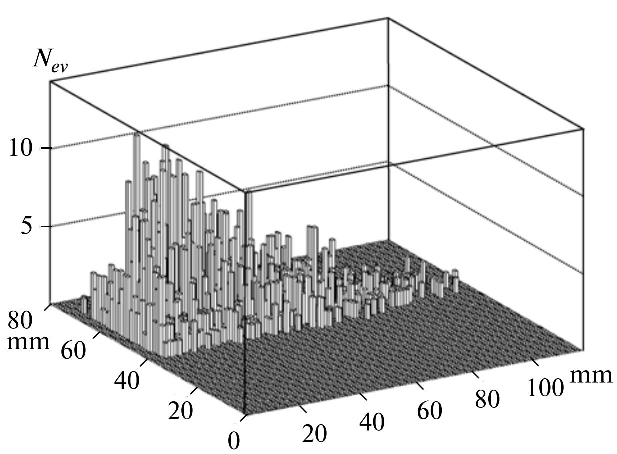

Fig. 6. Beam profile in the hammerlike decays; the bin size is 1 × 1 mm.

There is often a gap observed between the stopping point and the hammerlike decay itself. These "broken" events were attributed to the drift of thermalized ^{8}He atoms that resulted from the neutralization of ^{8}He nuclei. This effect is determined by the nature of ^{8}He, and these events are particularly reliably identified. Since ^{8}He nuclei dominate in the beam (~80%), the distribution of the hammerlike decays over the emulsion area can be presented jointly for all observed events, including 1413 "whole" and 1123 "broken" ones (Fig. 6). There is a uniform distribution of vertices in the vertical coordinate and a characteristic scatter, as a result of separation, in the horizontal coordinate.

The events that included at least one electron were further measured using the 90× KSM microscopes. The average length of the beam tracks for 136 whole events was $\langle L(^{8}\text{He})\rangle = 263 \pm 11$ μm at the root-mean-square scatter (RMS) 113 μm, and for 142 broken events it was 296 ± 10 μm at the RMS 118 μm. Since the difference in the parameters is insignificant, the distributions of ranges in these events are jointly depicted in Fig. 7. The SRIM simulation program [11] allows the kinetic energy of the ^{8}He nuclei that penetrated into the emulsion pellicle to be evaluated on the basis of the range measurements. Its average value is $\langle E(^{8}\text{He})\rangle = 29 \pm 1$ MeV at the RMS 10 MeV.

The substantially lower average ^{8}He energy and its larger spread at the entrance to the emulsion pellicle when compared with the value set by the fragment separator is due to the deceleration in the wrapping paper. The calculated average range in the emulsion $\langle L(^{8}\text{He})\rangle$ with allowance for the deceleration in 1 mm of the paper is about 280 μm [11]. In addition, the inhomogeneous structure of the paper contributes to the considerable spread of ranges $L(^{8}\text{He})$ (Fig. 7), which calculations fail to describe. Thus, the inhomogeneity of the light-proof paper turns out to be a factor that cannot be ignored and, at the same time, is difficult to take into account exactly. The given estimate of the effective paper thickness can be a reference for planning irradiation with other nuclei.

Coordinates of decay vertices and stops of decay α particles were determined for the hammerlike decays from 136 whole and 142 broken events. In broken events the decay coordinate was found by extrapolating the electron track to the hammerlike track. Thus, the emission angles and ranges of α particles were obtained.

Figure 8 shows the emission angle distribution of pairs of α particles. The average value of the angles is $\langle \theta_{2_\alpha} \rangle = (164.9 \pm 0.7)°$ at the RMS $(116 \pm 0.5)°$. A small kink in the hammerlike decays is determined by the momenta carried away by *eν* pairs. Figure 9 depicts the relation between the ranges L_α of the α particles from the hammerlike decays and the energies E_α found from the spline interpolation of the range–energy calculation within the SRIM model. The average of the α particle ranges is 7.4 ± 0.2 μm at the RMS 3.8 ± 0.2 μm, which corresponds to the average kinetic energy $\langle E(^{4}\text{He})\rangle = 1.70 \pm 0.03$ MeV at the RMS 0.8 MeV. The ranges L_1 and L_2 of α particles in pairs exhibit a distinct correlation (Fig. 10). The distribution of the range differences $L_1 - L_2$ (Fig. 11) has the RMS 2.0 μm.

Knowing the energy and emission angles of the α particles, we can obtain the α decay energy distribution $Q_{2\alpha}$. The relativistically invariant variable Q is defined as a difference between the invariant mass of the final system M^* and the mass of the primary nucleus M; i.e., $Q = M^* - M$. Here M^* is defined as a sum of all products of the fragment four-momenta $P_{i,k}$,

$$M^{*2} = \left(\sum P_j\right)^2 = \sum (P_i P_k).$$

The $Q_{2\alpha}$ distribution (Fig. 12) mainly corresponds to the decays of ^{8}Be nuclei from the excited 2^+ state. Its average value $\langle Q_{2\alpha}\rangle$, however, turned out to be slightly greater than expected, which results from a small tail in the region of large $Q_{2\alpha}$ that obviously does not fit into the description by the Gaussian function. Apply-

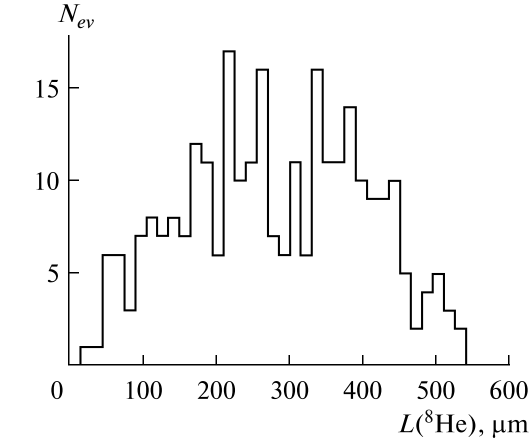

Fig. 7. Range distribution of the ^{8}He tracks in the emulsion.

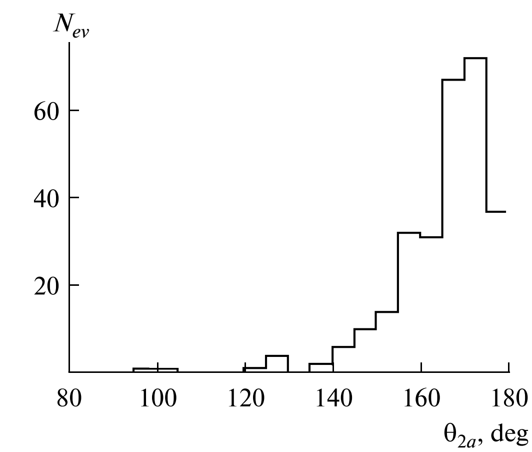

Fig. 8. Angle θ_{2_α} distribution in pairs of α particles.

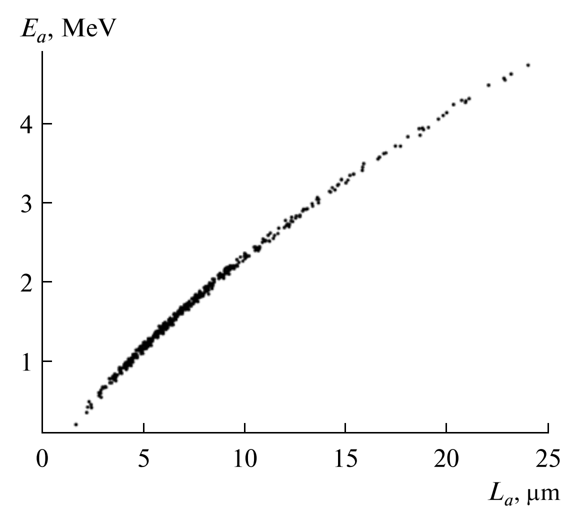

Fig. 9. Determination of the α particle energy from the measured ranges.

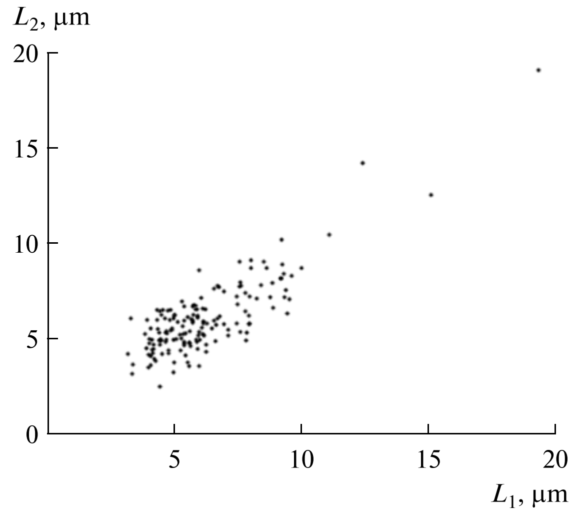

Fig. 10. Distribution of ranges L_1 and L_2 in pairs of α particles.

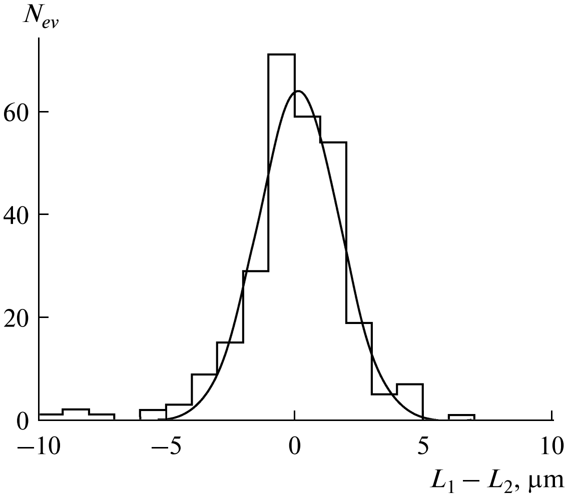

Fig. 11. Distribution of range differences $L_1 - L_2$ in pairs of α particles; the curve is the Gaussian function.

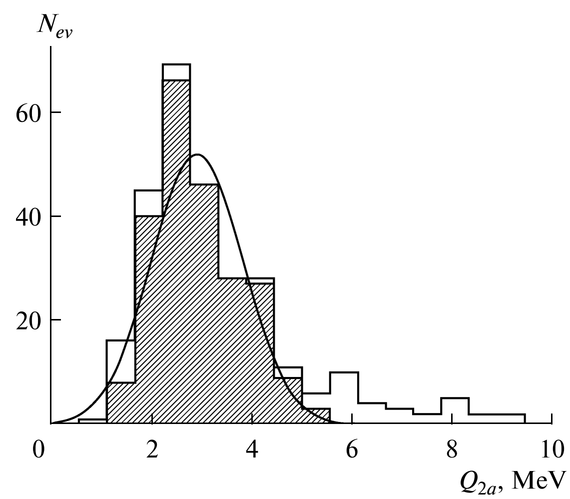

Fig. 12. Energy $Q_{2\alpha}$ distribution of α particle pairs; the hatched histogram satisfies the event selection conditions L_1 and $L_2 < 12.5$ μm. The curve is the Gaussian function.

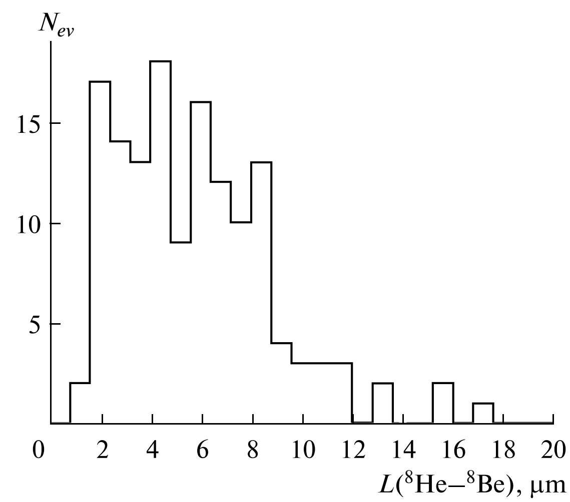

Fig. 13. Distribution of distances $L(^8He–^8Be)$ between the ^8He stopping points and the $^8Be(2^+)$ decay vertices in the broken events.

ing the selection criteria L_1 and $L_2 < 12.5$ μm and $\theta > 145°$, we obtain $\langle Q_{2\alpha} \rangle = 2.9 \pm 0.1$ MeV at the RMS 0.85 ± 0.07 MeV, which corresponds to the 2^+ state.

The reason why the tail arises in the $Q_{2\alpha}$ distribution is obscure and calls for further analysis. According to Fig. 10, the ranges L_1 and L_2 correlate at values greater than 12.5 μm as well. Therefore, an increase in ranges cannot be attributed to fluctuations of ranges due to recombination of He^{+2} ions. This fact should be taken into consideration in a comprehensive analysis.

The resolution of the nuclear track emulsion is enough to find the distances $L(^8He–^8Be)$ between the ^8He stopping points and the $^8Be(2^+)$ decay vertices in the broken events (Fig. 13). The average value $\langle L(^8He–^8Be) \rangle = 5.8 \pm 0.3$ μm at the RMS 3.1 ± 0.2 μm can be associated with the average drift length of thermalized ^8He atoms.

The observation of the drift indicates the possibility of generating radioactive ^8He atoms and pumping them out from sufficiently thin targets. The drift rate and length can be increased by heating the target. Extensive research in this direction with application to ^6He isotopes is under way [12, 13]. The prospect of accumulating considerable amounts of ^8He atoms exists. Radioactive ^8He gas can be used for measuring the ^8He half-life at a new level of accuracy and for the laser spectroscopy of ^8He. Of applied interest is the investigation of thin films by pumping ^8He atoms with their particular penetrating power and depositing them onto detectors.

CONCLUSIONS

This work demonstrates the capabilities of the recently reproduced nuclear track emulsion exposed to a beam of ^{8}He nuclei. The test experiment allowed radioactive ^{8}He nuclei to be independently identified by their decays as they stopped in the emulsion, the possibility of carrying out the α spectrometry of these decays to be estimated, and the drift of thermalized ^{8}He atoms in matter to be observed for the first time. The experiment proved the high purity of the beam of radioactive nuclei formed at the ACCULINNA facility with an energy ranging from 10 to 30 MeV/nucleon. The analysis of 278 decays of ^{8}He nuclei can be a prototype for investigating decays of ^{8,9}Li, ^{8,12}B, ^{9}C, and ^{12}N nuclei in which the ^{8}Be nucleus serves as a marker. The nuclear track emulsion can be used for the diagnostics of beams of radioactive isotopes.

The statistics of the hammerlike decays observed in this work is a small fraction of the flux of ^{8}He nuclei, and the measured decays constitute 10% of that fraction. This limitation was dictated by "reasonable" time and labor expenditure. At the same time the nuclear track emulsion with implanted radioactive nuclei offers the basis for using automatic microscopes and image-recognition programs, making it possible to hope for unprecedented statistics of analyzed decays. Thus, classical methodology can be synergistically combined with modern technologies.

ACKNOWLEDGMENTS

The authors are grateful to the project curator O.I. Orurk (Moscow); Yu.A. Berezkina, A.V. Kuznetsov, and L.B. Balabanova (Micron, Slavich, Pereslavl' Zalesskii) for making new samples of nuclear track emulsion available; A.S. Mikhailov (Moscow Cinematography and Video Institute) for methodological assistance in reproducing the nuclear track emulsion technology; N.G. Polukhina (FIAN) and A.I. Malakhov (JINR) for constant assistance in our work, and the technician G.V. Stel'makh (JINR) for making an appreciable contribution to the search for events.

The work was supported by the Russian Foundation for Basic Research, project no. 12-02-00067, and by grants from the Plenipotentiaries of the Governments of Bulgaria and Romania at JINR.

REFERENCES

1. C. F. Powell, P. H. Fowler, and D. H. Perkins, *Study of Elementary Particles by the Photographic Method* (Pergamon, London, 1959), pp. 465–472.
2. M. S. Swami, J. Schneps, and W. F. Fry, Phys. Rev. **103**, 1134–1135 (1956).
3. F. Ajzenberg-Selove, Nucl. Phys. A **490**, 1–266 (1988); TUNL, Nuclear Data Evaluation Project. http://www.tunl.duke.edu/NuclData/
4. The BECQUEREL Project. http://becquerel.jinr.ru/miscellanea/8 He/8 He.html
5. A. M. Rodin et al., Nucl. Instrum. Methods Phys. Res., Sect. B **204**, 114–118 (2003).
6. The ACCULINNA Project. http://aculina.jinr.ru/
7. Flerov Laboratory of Nuclear Reactions, U400M Accelerator Complex. http://flerovlab.jinr.ru/flnr/u400m.html
8. U. Rohrer, PSI Graphic Transport Framework based on a CERN-SLAC-FERMILAB version by K.L. Brown et al. http://aea.web.psi.ch/Urs_Rohrer/MyWeb/trans.htm
9. K. L. Brown et al., 1980 CERN Yellow Report 80-04.
10. Slavich Company. www.slavich.ru
11. J. F. Ziegler, J. P. Biersack, and M. D. Ziegler, *SRIM—the Stopping and Range of Ions in Matter* (SRIM Co, 2008); Particle Interactions with Matter, SRIM—The Stopping and Range of Ions in Matter. http://srim.org/
12. A. Knecht et al., Phys. Rev. C **86**, 035506 (2012).
13. T. Stora et al., Europhys. Lett. **89**, 32001 (2012).

Translated by M. Potapov